

The First 1-2 Gyrs of Galaxy Formation: Dropout Galaxies from $z \sim 3 - 6$

Garth Illingworth and Rychard Bouwens

UCO/Lick Observatory, Astronomy and Astrophysics Department, University of California, Santa Cruz, CA 95064

Abstract. The unique high-resolution wide-field imaging capabilities of HST with ACS have allowed the characterization of galaxies at redshift 6, less than 1 Gyr from recombination. The dropout technique, applied to deep ACS i , z images in the RCDS 1252–2927, GOODS and UDF-Parallel fields has yielded large samples of these objects, allowing a detailed determination of their properties (e.g., size, color) and meaningful comparisons against lower redshift dropout samples. The use of cloning techniques has enabled us to control for many of the strong selection biases that affect the study of high redshift populations. A clear trend of size with redshift has been identified, and its impact on the luminosity density and star formation rate can be estimated. There is a significant, though modest, decrease in the star formation rate from redshifts $z \sim 2.5$ out through $z \sim 6$. The latest data also allow for the first robust determination of the luminosity function at $z \sim 6$.

1 Introduction

The advent of the HST Advanced Camera, the ACS (Ford et al 2003) has greatly increased our ability to “watch galaxies form”. The sensitivity, resolution and excellent filter set have provided us with images from which large samples of high redshift galaxies can be derived. Of particular interest are those galaxies with red enough i - z colors to qualify as i -dropouts – galaxies at redshifts $z \sim 6$. Such objects have been the focus of a number of papers over the last year (e.g., Bouwens et al 2003b, Stanway et al 2003, Yan et al 2003, Dickinson et al 2004). Spectroscopic confirmation is beginning to appear (e.g., Bunker et al 2003, Dickinson et al 2004) but is challenging as Weymann et al (1998) demonstrated with their $z = 5.6$ object, which took over 6 hours on Keck.

The current frontier for high redshift objects is at $z \sim 6$ (the ACS UDF and NICMOS UDF-IR images together will likely extend the dropout sources to redshifts 7 and beyond, but the samples will be small). Rapid changes in the properties of high redshift galaxies must occur beyond $z \sim 6$ and so careful characterization of objects even those separated by small intervals of time, is a well-justified goal. Given this, there is great value in having large samples of $z \sim 3 - 5$ objects to contrast with $z \sim 6$ galaxies. Though only 0.2 – 1.0 Gyr later in cosmic history, $z \sim 3 - 5$ object samples are larger and much better characterized, providing key information on evolutionary changes in high redshift galaxies.

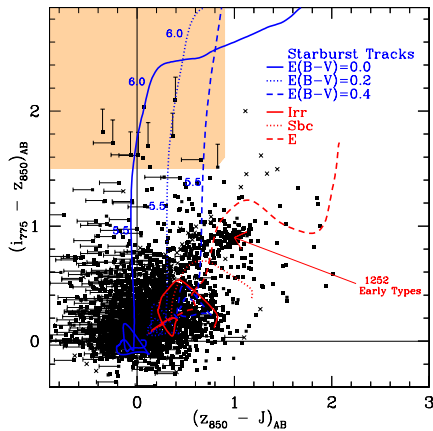


Fig. 1. Selection of i -dropouts in the i - z - J two-color plane. This example is for the HST ACS from the RCDS 1252–2927 field (Rosati et al 1998). The selection limits (particularly the $(i-z) > 1.5$ cut – see Bouwens et al 2003b) returns $z \sim 6$ galaxies with little contamination (an estimated 11% contamination rate).

2 Fields and Object Selection

While data from several fields have been used to identify high redshift dropouts, three fields have stood out for their value for dropout studies over the last year – namely the RCDS 1252–2927 field, the GOODS fields, and the UDF–parallels (UDF–Ps). All have excellent HST ACS i_{775} and z_{850} data, while the GOODS and the UDF–Ps fields also have deep B_{435} and V_{606} data. The excellent IR data (Lidman et al 2004) in RCDS 1252–2927 also makes a substantial contribution to the selection of i -dropouts, helping to establish the degree of contamination in the samples.

The selection of i -dropouts is shown in Fig 1 for the RCDS 1252–2927 field (from Bouwens et al 2003b). The ACS data reaches typically to $z_{850,AB} \sim 27.3$ mag (6σ), while the ground-based IR data goes impressively deep, down to $J_{AB} = 25.7$ and $Ks_{AB} = 25.0$ mag (5σ). The fraction of $z \sim 6$ objects in the IR coverage in RCDS 1252–2927 is impressively small (0.3%), only 12 out of ~ 3000 galaxies. Even so the estimated contamination is only about 11%. A number of these candidates have been observed with Keck and the VLT and confirmed to be at $z \sim 6$. A total of 23 $z \sim 6$ galaxies are found in four ACS pointings of the RCDS 1252–2927 field, giving a surface density of 0.5 ± 0.2 i -dropouts per square arcmin to $z_{AB} = 26.5$ mag. The objects are very small, though all are resolved, with typical half-light radii of $0.15''$ or ~ 0.9 kpc. The $z \sim 6$ objects reach down to $\sim 0.3L_{*,z=3}$ (Steidel et al 1999).

Two of the brighter i -dropouts from the RCDS 1252–2927 field are shown in Fig 2, along with their location in the two-color plane, and SED fits that are used to establish the redshifts. The ACS i and z data from the HDF–N also allowed for a search for i -dropouts. A reassuring result was that the Weymann et al (1998) object in the HDF–N, spectroscopically verified to be at $z = 5.60$, was very close to meeting our i -dropout criterion (its $i-z = 1.2$ color was just a little too blue). While not a true i -dropout, it suggested that our selection was

yielding bona-fide high redshift objects. Other spectroscopic results from Bunker et al (2003) and Dickinson et al (2004), and our own ongoing Keck programs, have only served to strengthen our confidence in the dropout approach.

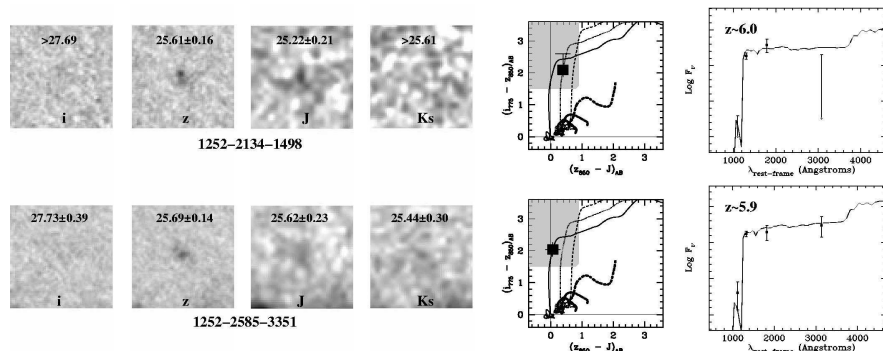


Fig. 2. Images ($3'' \times 3''$) in i , z , J , Ks of $z \sim 6$ objects, along with two-color schematics (showing starburst tracks as a function of redshift for different reddenings - see Fig 1), and starburst galaxy SEDs (10^8 Gyr), with the best fit redshift. The sources are all in RCDS 1252-2927. The magnitudes given for the sources are AB magnitudes.

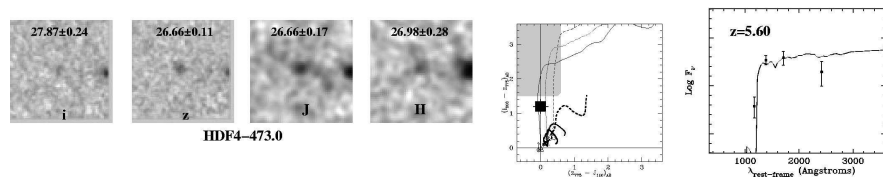


Fig. 3. As in Fig 2, but for the Weymann et al (1998) galaxy in the HDF-N whose redshift was measured to be $z = 5.6$ from over 6 hours of integration with the LRIS spectrograph on Keck. The redshift determined from the photometric data was also $z = 5.6$.

While the RCDS 1252-2927 field provided a significant sample of i -dropouts (with a good assessment of the contamination from the deep VLT IR data), the best samples of brighter dropouts come from the two HST ACS GOODS fields, CDF-S and HDF-N (see Giavalisco et al 2004). From these fields, Bouwens et al (2004b) derived a large number of B -, V - and i -dropouts, augmenting them with a smaller but very useful sample of U -dropouts from the HDF-N and HDF-S fields so that a self-consistent differential analysis could be applied across a large redshift range, $z \sim 3$ to $z \sim 6$. Even with relatively conservative selection criteria, Bouwens et al (2004b) derive 1235 $z \sim 4$ B -dropouts, 407 $z \sim 5$ V -dropouts, and 59 $z \sim 6$ i -dropouts. These samples go as faint as 0.2, 0.3, 0.5

$L_{*,z=3}$ (using the Steidel et al 1999 value for $L_{*,z=3}$), respectively, with 10σ limiting magnitudes of 27.4 in the $i_{775,AB}$ band and 27.1 in the $z_{850,AB}$ band.

The large samples and wide areal coverage of the GOODS fields are nicely complemented by the two UDF-parallel fields (UDF-Ps) obtained in parallel with the deep NICMOS images of the UDF. These fields have overlapping ACS images on a $45''$ grid with 9 orbits each in B and V, 18 orbits in i and 27 orbits in z (as well as 9 orbits with the grism). They reach impressively faint, to 28.8, 29.0, 28.5 and 27.8 mag (10σ) in B_{435} , V_{606} , i_{775} , and z_{850} AB-mag, respectively – or to 0.1 – $0.2L_{*,z=3}$. The UDF itself will be an impressive addition to these fields, taking the limits to $< 0.1L_{*,z=3}$.

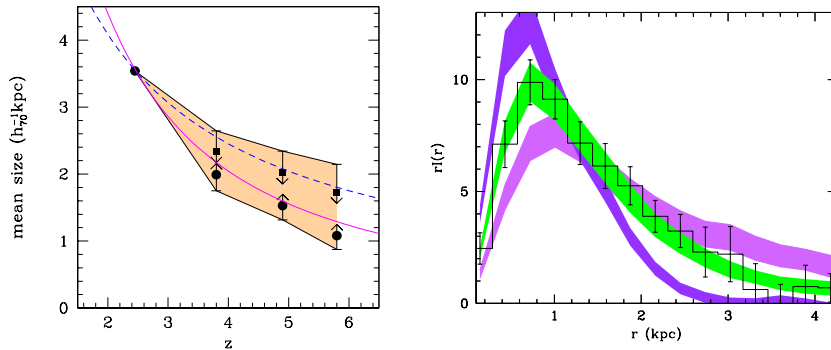


Fig. 4. (Left) Size evolution of $1 - 2L_{*,z=3}$ galaxies derived from composite radial flux profiles for objects with redshifts from $z \sim 2.5$ to $z \sim 6$ (Bouwens et al 2004b). The solid black circles (1σ errors) give the observed sizes with redshift, and should be a lower limit. The solid black squares are expected to be upper limits and show the evolution obtained by bootstrapping the sizes from $z \sim 2.5$, comparing each sample with the one adjacent to it in redshift (see Bouwens et al 2004b for more detailed argumentation). A clear evolution towards smaller size is observed with redshift, consistent with the scalings predicted from hierarchical models ($H(z)^{-1} \sim (1+z)^{-3/2}$ for fixed circular velocity [solid line] and $H(z)^{-2/3} \sim (1+z)^{-1}$ for fixed mass [dashed line]). (Right) The mean radial flux profile for the 10 brightest i -dropouts in the UDF-Ps (histogram) compared with “cloned” projections of the HDF-N and HDF-S U -dropout sample scaled in size as $(1+z)^m$, where $m = 0, -1.5$ and -3 ; $m = -1.5$ is the best fit (Bouwens et al 2004a).

3 Results

A major issue with deriving the evolution of galaxy properties at high redshift is systematic error – primarily through the many selection effects that can influence the nature of the samples, even when derived from very similar datasets. Of

these the $(1+z)^4$ surface brightness dimming is the dominant effect, but many others affect the derived samples (e.g., size evolution, color evolution, definition of selection volumes, data properties as a function of redshift, filter band, and instrument, etc.). To treat these effects, we compare our highest redshift samples with “cloned” projections of our lower redshift samples (e.g., Bouwens et al. 1998; Bouwens et al. 2003a), allowing us to contrast intrinsic evolution from changes brought about by the selection process itself.

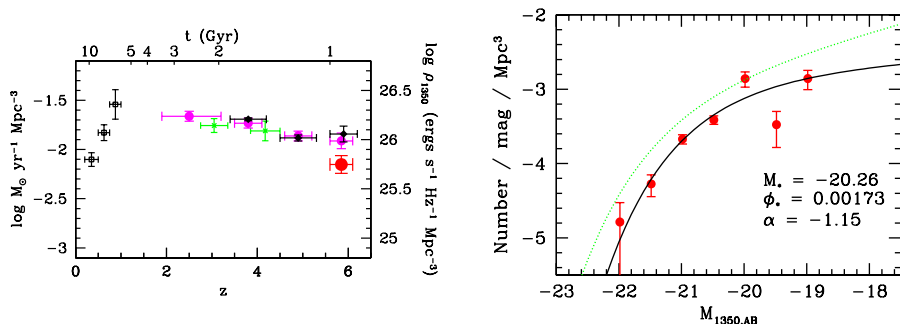


Fig. 5. Star formation rate evolution (dust-free) with redshift and age (top), integrated down to $0.2L_{*,z=3}$ (rest-frame UV continuum luminosity density on the right vertical axis for the high redshift values). Note the small Δt from $z \sim 6$ to $z \sim 3$. A Salpeter IMF is used to convert the luminosity density to SFR (see Madau et al 1998). (Left) The four solid circles from $z = 2.5$ to $z = 6$ are the values from the GOODS data (Bouwens et al 2004b). Other determinations are Lilly et al (1996 – open squares), Steidel et al (1999 – crosses), Bouwens et al (2004a – solid circles at $z = 6$) and Giavalisco et al (2004 – solid diamonds). The Thompson et al (2001) values are similar to those shown here. The low point at $z = 6$ includes the effect of size evolution on the $z \sim 6$ Bouwens et al (2004a) value (indicating how significant this effect can be). (right): The rest frame continuum UV (at 1350 Å) luminosity function at $z \sim 6$ from the GOODS field (for $M_{1350,AB} < -19.7$) and the UDF-Ps. The best fit values for a Schechter luminosity function are shown on the figure. The Steidel et al (1999) $z \sim 3$ luminosity function (dotted line) is also shown. The Steidel luminosity function had a best fit faint end slope $\alpha = -1.6$. Such a slope is also consistent with our $z \sim 6$ data.

One of the key results is that of size evolution. This is demonstrated in Fig 4a for the GOODS fields (see also Ferguson et al 2004). The deeper UDF-Ps provide stronger and even more conclusive evidence for this (see Bouwens et al 2004a), as well as indicating that the best fit appears to be with $(1+z)^{-1.5}$ (Fig 4b).

A major goal of these studies is to extend the constraints on the luminosity density and the star formation rate with redshift to higher redshifts $z \sim 6$ and beyond. A related goal is to improve the constraints at lower redshifts ($z \sim 2-5$). These new datasets are proving to be of great value for these two goals. Fig 5a

gives the most recent estimate of the (dust-free) star formation rate (including the effect of size evolution) out to $z \sim 6$.

Another major development over the last year is that the HST ACS data is now of sufficient quality and depth that a luminosity function can be derived to significantly fainter than L_* , as was recently done by Bouwens et al. (2004a) with the GOODS + UDF-Ps data (Fig 5b). The UDF will extend this luminosity function one magnitude fainter.

4 Summary

There has been a remarkable growth in the number of objects known at high redshifts ($z \sim 6$) since the HST Advanced Camera came into operation after servicing mission SM3B. Not only are large numbers of sources being detected at high redshift, but the development of new techniques for detecting, characterizing and comparing high redshift objects from photometric datasets has led to many quantitative results on the nature and evolution of galaxies in the first $\sim 1 - 3$ Gyrs.

Acknowledgments We would like to thank the organizers for an excellent meeting in a great place. We acknowledge the remarkable advances that have come about because of HST and its amazing imagers, and regret the decision to cancel SM4 that will lead to the premature death of HST. We owe a lot to our team members on the ACS GTO team and the UDF-IR team, and particularly the PIs, Holland Ford and Rodger Thompson. Support from NASA grant NAG5-7697 and NASA/STScI grant HST-GO-09803.05-A is gratefully acknowledged.

References

1. Bouwens, R., Broadhurst, T. and Silk, J. 1998, ApJ., **506**, 557.
2. Bouwens, R., Broadhurst, T., & Illingworth, G. ApJ., **593**, 640 (2003a).
3. Bouwens, R. J., et al. ApJ., **595**, 589 (2003b).
4. Bouwens, R. J. et al. ApJ., in press (2004a).
5. Bouwens, R. J. et al. ApJ., in submission (2004b).
6. Bunker, A. J., Stanway, E. R., Ellis, R. S., McMahan, R. G., & McCarthy, P. J. MNRAS, **342**, L47 (2003).
7. Dickinson, M., et al. ApJ., **600**, L99 (2004).
8. Ferguson, H.C., et al. ApJ., **600**, L107 (2004).
9. Ford, H. C. et al. Proc. SPIE, **4854**, 81 (2003).
10. Giavalisco, M., et al. ApJ., **600**, L93 (2004).
11. Lidman, C., et al. A.& A., in press (2004).
12. Lilly, S.J., Le Fevre, O., Hammer, F., & Crampton, D. ApJ., **460**, L1 (1996).
13. Madau, P., Pozzetti, L. & Dickinson, M. ApJ., **498**, 106 (1998).
14. Rosati, P., et al. ApJ., **492**, L21 (1998).
15. Stanway, E. R., Bunker, A. J., & McMahan, R. G. MNRAS, **342**, 439.
16. Steidel, C. C., Adelberger, K. L., Giavalisco, M., Dickinson, M. and Pettini, M. ApJ., **519**, 1 (1999).
17. Thompson, R. I., Weymann, R. J., & Storrie-Lombardi, L. J. ApJ., **546**, 694 (2001).
18. Weymann, R. J., et al. ApJ., **505**, L95 (1998).
19. Yan, H., Windhorst, R. A., & Cohen, S. H. ApJ., **585**, L93 (2003).